Article:

Jiang, W, Xiao, J, Yuan, D et al. (3 more authors) (2018) Design and experiment of thermoelectric asphalt pavements with power-generation and temperature-reduction functions. Energy and Buildings, 169. pp. 39-47. ISSN 0378-7788

https://doi.org/10.1016/j.enbuild.2018.03.049

Design and experiment of thermoelectric asphalt pavements with power-generation and temperature-reduction functions

Wei JIANG [a,*], Jingjing XIAO [b], Dongdong YUAN [a], Hehe LU [a], Shudong XU [a], Yue HUANG [c]

[a] Key Laboratory for Special Area Highway Engineering of Ministry of Education, Chang'an University, South 2nd ring road Middle Section, Xi'an, Shaanxi, 710064, China

[b] School of Civil Engineering, Chang'an University, South 2nd ring road Middle Section, Xi'an, Shaanxi, 710064, China

[c] Institute for Transport Studies (ITS), University of Leeds, 34-40 University Road, Leeds, LS2 9JT, United Kingdom

* Corresponding author. E-mail address: jiangwei_029@sina.com (W. Jiang).

ABSTRACT: Asphalt pavements tend to absorb solar energy and accumulate heat, which results in several negative effects. They contribute to the urban heat-island effect, plastic deformation of pavements, and aging of asphalt materials. One solution is to convert or transfer the pavement heat. A brand new road thermoelectric generator system (RTEGS) is designed for this purpose. The system added three modules to the traditional asphalt pavement structure: heat-conduction, thermoelectric-conversion, and cold-end cooling. The modules convert heat absorbed in asphalt pavements to electrical energy and reduce the pavement surface temperature. Field testing of the new system subject to a full seasonal change (half a year) was conducted. The data of temperature reduction and voltage output in a field environment were obtained. The results showed that the system reduced the pavement surface temperature by 8–9°C in hot seasons, and the electrical output from an asphalt pavement of size 300 mm × 300 mm × 100 mm reached 0.564 V. At this output, a 10,000 m^2 (1 km long and 10 m wide) pavement area would generate about 33 kWh of electrical energy in a single day in the summer, not considering the scale effects of the RTEGS. The system provides a new approach to alleviate the urban heat-island effect, and to convert and utilize solar heat absorbed in asphalt pavement.

Key words: Asphalt pavement, Energy harvesting, Thermoelectric, Heat-island effect, Temperature reduction

1 Introduction

Asphalt pavements are the primary type of urban roads and highways on account of their low cost, less tyre-road noise as well as riding quality. However, black asphalt pavement materials tend to absorb solar radiation energy and accumulate heat. The pavement temperature can reach 60°C or higher in summer [1], bringing negative effects to the environment and the pavements themselves. These effects include: 1) Aggravating the urban heat-island effect [2-4]. Roads generally account for over 30% of a city's area [5]. The ratio can be higher in big cities [6-8]. In summer, a large amount of heat is absorbed and accumulated by asphalt pavements in the daytime [9]. The pavement temperature is generally 20°C higher than the environmental temperature at mid-day during sunny summer months. At night, the heat absorbed by pavement is transmitted to the surroundings. For above reasons, asphalt pavements are the main cause for the urban heat-island effect. 2) Exacerbating pavement rutting and other heat induced damage [10]. Under high temperatures, asphalt mixtures are prone to irreversible plastic deformation under repetitive wheel loadings. Rutting, shoving and upheaval can occur, affecting functionality and safety of the pavement [11-13]. 3) Accelerating the thermal aging of asphalt pavement materials. Continuous high temperatures increase the oxidation of bitumen and the volatilization of its light components. The ductility of bitumen decreased as a result of aging. Crack- and fatigue-resistance of the bitumen is thus reduced, and the service life of pavements shortened [14-16].

For the above reasons, temperature within the asphalt pavement needs to be reduced in high-temperature seasons from the perspectives of the environment, pavement performance, and materials durability [17, 18]. Accordingly, researchers and engineers have developed light-colored pavements, water-retentive pavements and permeable pavements [19]. The mechanism for reducing temperature of light-colored pavements is to increase heat reflectivity of road surface materials [20, 21]. The water-retentive pavements have the capability of absorbing and preserving water from rainwater or artificially sprayed water. The temperature of pavement will be reduced by the water evaporation during high temperature seasons [22]. The permeable pavements, which is connected with the natural ground due to its large inter-connected void, reduce road and ambient temperature by improving moisture circulation between the underground and aboveground spaces [18, 23].

Some related projects have been implemented successfully. Toraldo et al. discovered that lighter-colored pavements can have temperatures 14°C lower than those of conventional asphalt pavements [24], and Karasawa found that temperatures of light-colored and water-retentive concrete pavements can be 7.2–16.6°C lower [25]. Yamagate et al. concluded that the temperature of water-retentive pavements can be reduced by 8°C on average in the daytime and 3°C at night by spraying recycled water onto them, and thus alleviate the urban heat-island effect [26]. The ambient temperature can be effectively reduced as a result of reduction in temperature of the road surface [27]. Santamouris et al. investigated the cooling effect of reflective pavements in an urban park. Their results showed that, reflective pavements contribute to the reduction of the ambient temperature during a typical summer day, by up to 1.9°C while the surface temperature in the park was reduced by up to 12°C [28].

On the other hand, heat retained in the pavement can be utilized as energy from the perspective of resource conservation [29-32]. There are usually two major approaches. One is to directly collect solar energy from the pavement surface and convert it to electrical energy [33]. A common method is to pave photovoltaic panel on the pavement surface [34-36]. For example, the TNO company in the Netherland paved a crystalline silicon solar panel at 10 mm depth on a bicycle lane located in Krommenie, a town northwest of Amsterdam [37]. Another method is to embed pipelines in pavement structure. Flowing liquids in the pipelines will absorb pavement heat and take it out of the pavement, which can then be utilized [38, 39]. For example, Sullivan proposed a pavement-heat utilization system composed of asphalt pavement layers and water pipes [40]. At high temperatures in summer, water in pipes can absorb and transfer the pavement heat. The heat is stored in soil or storage tanks, which can be used in winter to melt snow on the road and heat nearby buildings. Hasebe et al. laid water pipes under asphalt pavements to absorb heat, which was used for electric power generation [41]. It is worth noting that most of these researches used thermal (and not electric) conversion from heat stored in roads.

Overall, a variety of methods can be used to reduce pavement temperatures. Yet very few approaches to utilize pavement heat have been discussed. This is because pavement heat can be dispersed easily, and is hard to collect and utilize. As a result, very few literatures on the comprehensive study of pavement temperature reduction and heat utilization are found. To fill the research gap, we designed a novel set of road thermoelectric generator system (RTEGS) to reduce pavement surface temperature and utilize pavement heat. The system can partially convert pavement heat to electrical energy, reducing pavement temperature while utilizing solar energy stored in pavement. A field experiment was conducted to test the effectiveness of RTEGS in generating power and reducing temperature. Findings from this study will provide a new approach to alleviate urban heat-island effect and utilize asphalt pavement heat.

2 RTEGS Design

The main concept of RTEGS design was to convert the heat absorbed by asphalt pavements to electrical energy. Resultantly, the pavement temperature would decrease. In addition to materials used in the conventional asphalt pavement, RTEGS included heat-conduction, thermoelectric-conversion, and cold-end cooling modules. Details of each module are described as follows:

(1) The main function of the heat-conduction module was to collect heat absorbed in pavement and transfer it outside the pavement structure. To attain this, a highly efficient vapor chamber was embedded in pavement at a depth of 20–30 mm. One end of the vapor chamber was buried in the pavement, and the other end was exposed outside the pavement.

(2) The role of the thermoelectric-conversion module was to convert the pavement heat energy from the vapor chamber into electrical energy. To achieve this, a thermoelectric generator (TEG) was arranged on the exposed end of the vapor chamber. The TEG could convert heat energy to electrical energy. The premise was that a temperature difference existed between the two sides (cold and hot) of TEG. Generally, the larger the temperature difference, the higher the voltage output is. To maintain a temperature difference, the hot side of the TEG was connected to the exposed end of the vapor chamber. In this way, the pavement heat was continuously transferred to the hot side of the TEG.

(3) The cold-end cooling module was designed to reduce the temperature of the cold side of the TEG, and therefore to increase the voltage outputs of the TEG. The cold-end cooling module could use

air or water for cooling. Generally, water cooling is more effective. Therefore, a water tank was installed at the cold side of the TEG. The bottom of the tank was made of a material with good thermal conductivity, such as vapor chamber or aluminum, and was bonded to the cold side of the TEG. The side walls of the tank were made of materials with good heat-dissipation performance. A shading board was erected on the outside of the tank to avoid direct sunshine that would increase the water temperature.

When the asphalt pavement temperature was increased by solar radiation, the heat would be transferred to the hot side of the TEG by the vapor chamber, creating a temperature difference between the hot and cold sides, and a voltage output would be generated, while the pavement temperature was reduced. In normal conditions, the asphalt pavement temperature was generally higher than the environmental temperature [32]. The mechanism of RTEGS was to make use of the temperature difference and to realize the conversion of heat energy to electrical energy by using the TEG. Fig. 1 illustrates the design of the RTEGS.

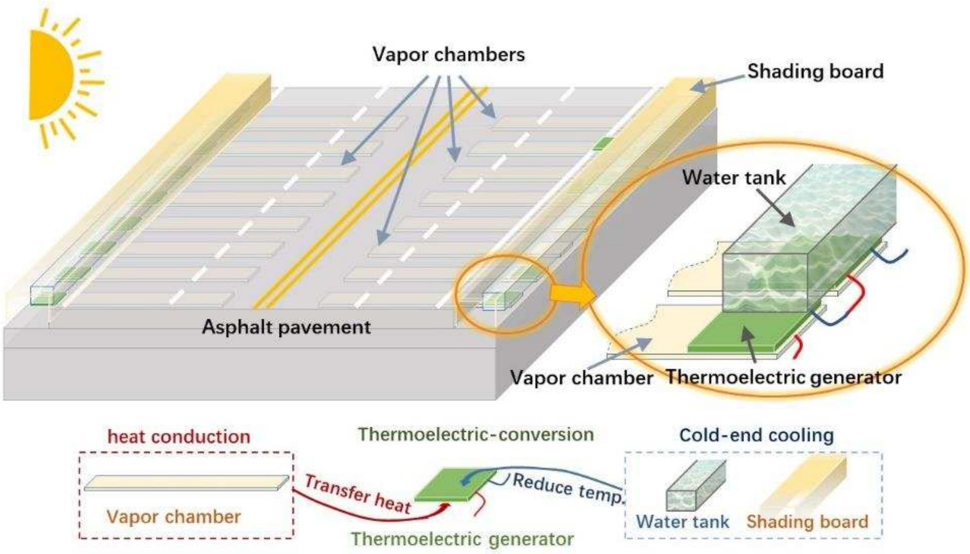

Fig. 1. Schematic of RTEGS design.

3 Experiment materials and method

3.1 Experiment materials

(1) Pavement structure and materials

The asphalt pavement model in this experiment used a double-layer slab specimen with a size of 300 mm × 300 mm and 100 mm thick. The top layer was SBS (styrene–butadiene–styrene) modified asphalt concrete (AC-13) with 40 mm thickness. The bottom layer was asphalt concrete (AC-20) with 60 mm thickness. Both layers were made of conventional asphalt pavement materials.

(2) Heat-conduction materials

Aluminum vapor chambers (Fig. 2a) were used as the heat-conduction module. One reason for using aluminum was their good pressure-bearing capacity. The aluminum vapor chamber can bear a uniform pressure of 4 MPa, which is higher than the loading requirements for traffic. Also, with a heat transfer coefficient of 106 W/m·K, aluminum vapor chambers have good heat-transfer performance. The aluminum vapor chamber used in our experiment was 3 mm thick, 300 mm long, and 60 mm wide. As shown in Fig. 2b, they were evenly arranged in the slab specimen at 20 mm depth with 200 mm embedded within the specimen and 100 mm exposed outside the specimen.

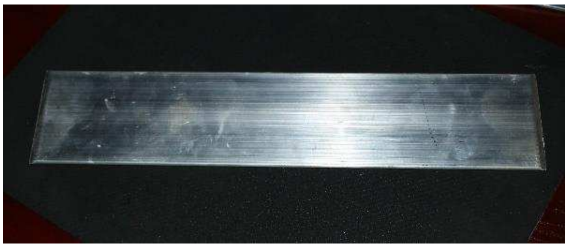

(a) Aluminum vapor chamber

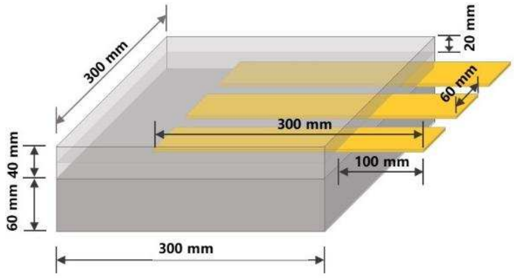

(b) Aluminum vapor chambers arrangement

Fig. 2. Aluminum vapor chamber and their arrangement in the slab specimen.

(3) Thermoelectric-conversion module

TEG-199 (Fig. 3a) used 199 pairs of thermoelectric components inside as the thermoelectric-conversion module. The hot side of the TEG was bonded to the exposed end of the aluminum vapor chamber on one side of the specimen by thermally conductive silica gel.

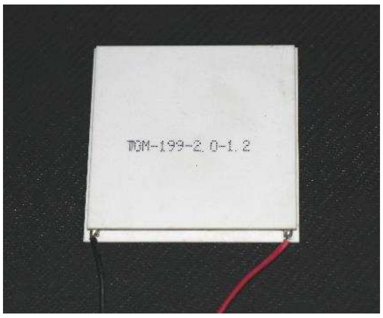

(a) TEG.

(b) Water tank

Fig. 3. TEG and Water tank.

(4) Cold-end cooling module

An organic glass water tank (Fig. 3b) was used to reduce the temperature of the cold side of TEG. The water tank was 350 mm long, 150 mm wide, and 160 mm high. The bottom of the tank was an aluminum vapor chamber, which could exchange heat efficiently between the TEG and the water in the tank. The tank's sidewalls were heat sinks that could exchange heat between the water and the air, keeping the water temperature consistent with the environmental temperature. The cold side of the TEG was bonded with the aluminum vapor chamber on the bottom of the water tank by thermally conductive silica gel. In field test, a shading board was used above the water tank to avoid direct sunshine that would increase the water temperature.

3.2 Testing methods

Field testing was conducted in Xi'an City, China, at 107.40–109.49° east longitude and 33.42–34.45° north latitude, where the climate is temperate with four distinct seasons. The highest temperature in summer can reach 40°C, and the lowest temperature in winter is generally −5°C. The average annual relative humidity is about 70%. The climate is representative of several main cities in China of similar size, population and land use. Fig. 4a and Fig. 4b illustrate the mean monthly high and low temperature, total solar irradiance and rainfall in Xi'an [42]. In field test, the slab specimen was placed outdoor. The TEG generated voltage under the solar radiation. A data-acquisition instrument was used to collect data.

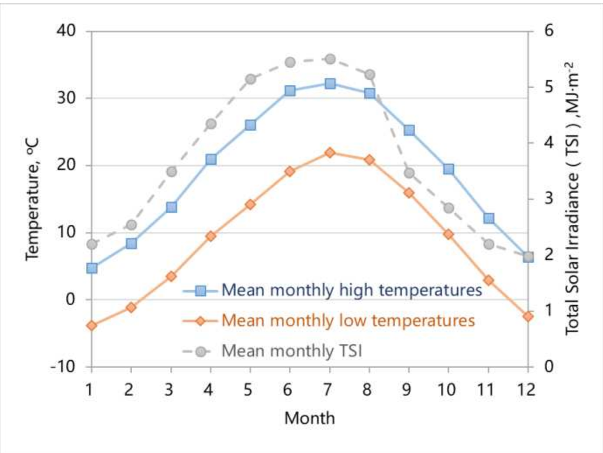

(a) Mean monthly high and low temperature, total solar irradiance

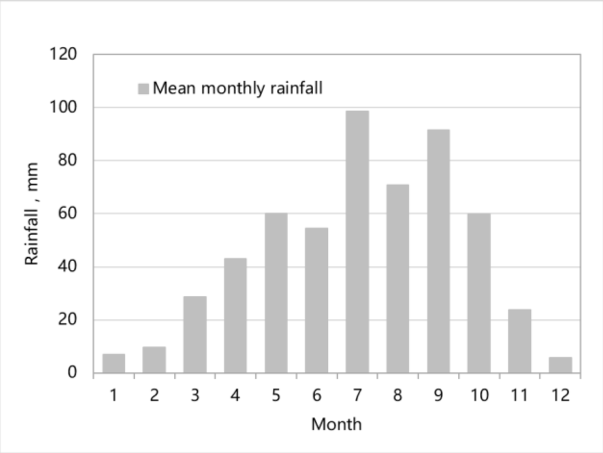

(b) Mean monthly rainfall

Fig. 4. Mean monthly high and low temperature, total solar irradiance and rainfall in Xi'an.

An Avio R300 thermal infrared imager was used to capture the surface temperature of the specimen every 10 minutes. The average temperature obtained by the infrared imager was used in data analysis. A PT100 temperature sensor and a data-acquisition instrument were used to collect the water temperature in the water tank. A mobile weather station was used to measure the environmental temperature. As shown in Fig. 5a, to reduce the heat exchange between the specimen and the surroundings, the specimen was wrapped with cotton heat insulator, and a wood panel was placed under the bottom of the specimen to separate it from the ground.

In order to analyze the effects of RTEGS on the pavement temperature, a conventional slab of the same size was fabricated using the same materials as the RTEGS specimen. The surface temperatures of the RTEGS specimen and the conventional slab were compared in the same field conditions. Testing was conducted from February to July 2017. A series of environmental temperatures in a full seasonal change were collected. Due to weather conditions in the field, not all days (the same day in every month) were suitable for measurement. As shown in Table 1, six testing days were selected for data analysis. These days were in similar intervals. They were all sunny during measurement and could be considered representative. Continuous observations and measurements of the temperature and voltage output were conducted on the RTEGS and conventional specimens. The duration of solar radiation changes with the season, thus data collection times varied slightly in different months. The data collection took place from 8:00 am to 10:00 pm from May to July, since solar radiation is longer during this season. The data collection was from 8:00 am to 7:00 pm from February to April, since solar radiation is relatively shorter in this season.

Table 1

Weather conditions of six testing days.

Date	Air temperature (ºC)	Peak radiation Intensity (W/m^2)	Weather	Wind direction	Wind scale
Feb. 24th, 2017	0-11	779	Sunny	West	1
Mar. 22nd, 2017	5-16	902	Cloudy	Southwest	3

Apr. 22nd, 2017	8-25	992	Sunny	West	2
May 26th, 2017	18-32	1038	Sunny	North	3
Jun. 26th, 2017	23-35	1022	Sunny	Southeast	2
Jul. 24th, 2017	27-40	999	Sunny	South	1

An iodine-tungsten lamp was used for indoor test, to simulate the solar radiation to heat the slab specimens, as shown in Fig. 5b. The temperatures (specimen surface and water) and the testing period were in a better-controlled environment compared with field testing.

(a) Field testing of RTEGS specimen.

(b) Indoor testing

Fig. 5. Field and indoor testing of RTEGS specimen.

4 Testing results

4.1 Power-generation

Fig. 6 illustrates the voltage output of the RTEGS specimen in the six testing days from February to July. The change of the voltage outputs over time exhibited a parabolic shape. The voltage outputs increased from about 10:00 am to 3:00 pm, and then decreased. Environmental conditions in different seasons significantly affected the voltage outputs. In May, June, and July when temperatures and solar radiation were higher, voltage output of the RTEGS specimen was higher and of longer duration. For example, on July 24, the measured peak voltage output was 0.564 V. Voltage outputs greater than 0.3 V lasted for more than 8 hours. In February, March and April when temperatures and solar radiation were lower, voltage outputs of the RTEGS specimen was smaller, and the voltage outputs period was shorter. For example, on February 24, the measured peak voltage output was 0.275 V.

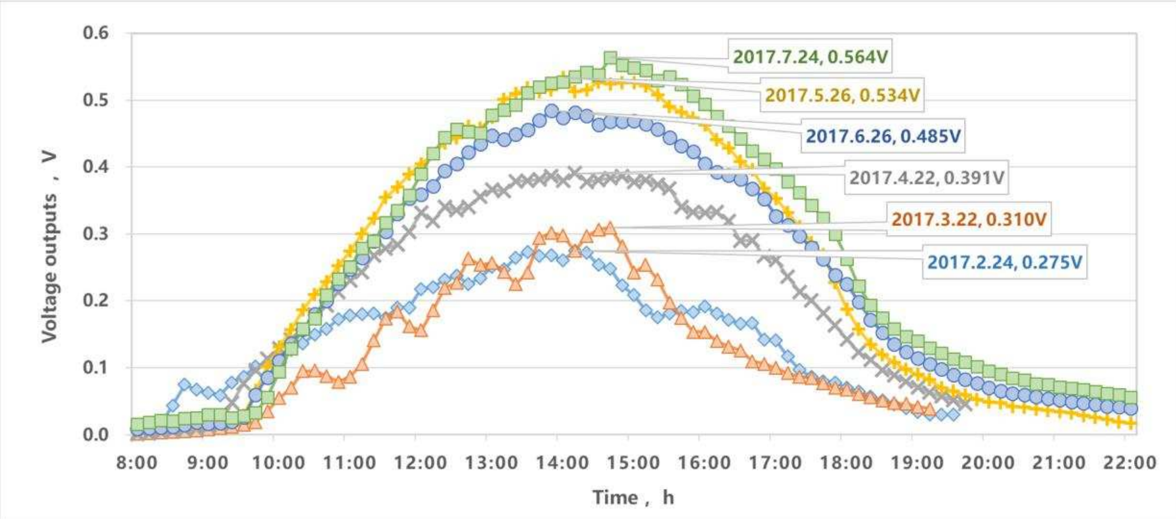

Fig. 6. Voltage outputs of the RTEGS specimen in different seasons.

The temperature difference between the specimen surface and the water in the tank can be controlled through the indoor test, in order to further analyze the influencing factors of the power generation. By adjusting the height of the light source, the surface temperature of the specimen was kept at 40°C; the temperature of the water in the sink can be kept at 20°C, 25°C and 30°C. The power generation of the RTEGS was measured at the temperature difference of 10°C, 15°C and 20°C, respectively. The effects of temperature difference and TEG number on voltage output of the RTEGS specimen are shown in Fig. 7. It can be seen that the voltage outputs of the system increase with an increase in temperature difference and the quantities of TEG, and there is a positive linear relationship between the voltage outputs and the temperature difference.

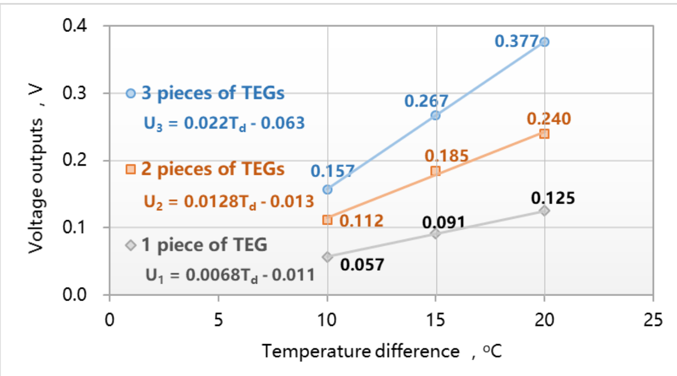

Fig. 7. Effects of temperature difference and TEG number on voltage output of the RTEGS specimen.

where U_i is the voltage outputs for i piece(s) of TEG(s); T_d is the temperature difference between the specimen surface and water in the tank.

4.2 Temperature-reduction

Fig. 8 illustrates the temperature of the RTEGS and conventional specimen in the six testing days from February to July 2017. The surface temperatures of the RTEGS specimen were significantly lower than those of the conventional specimen. In May, June, and July when temperatures and solar radiation were higher, temperature reduction in the RTEGS specimen was obvious. Peak reduction reached 8–9°C, and the reduction period was longer. For example, on May 26 (Fig. 8d), June 26 (Fig. 8e), and July 27 (Fig. 8f), temperature reduction above 5°C in the RTEGS specimen lasted for 7 hours, and temperature reduction above 3°C lasted for approximately 11 hours. In February, March, and April when temperatures and solar radiation were lower, the magnitude of temperature reduction in the RTEGS specimen was small. The maximum reduction was around 3–4°C, and the reduction was of short duration. For example, on February 24 (Fig. 8a), March 22 (Fig. 8b) and April 22 (Fig. 8c), the temperature reduction above 2°C lasted for approximately 3 hours. These magnitudes of temperature reductions are compatible with the pavement functionality requirements for different seasons. The pavement temperature needs to decrease significantly in summer to reduce plastic deformation and the urban heat-island effect, whereas in winter there is no need for reducing the pavement temperature.

In addition, as shown in Fig. 8, the temperature generally reached peak value between 2:00 pm and 3:00 pm. The maximum temperature difference between the two specimens occurred later, generally between 4:00 pm. and 6:00 pm. The results indicated that the temperature reduction by the RTEGS was lagging by approximately 2 to 3 hours behind the time of peak temperature.

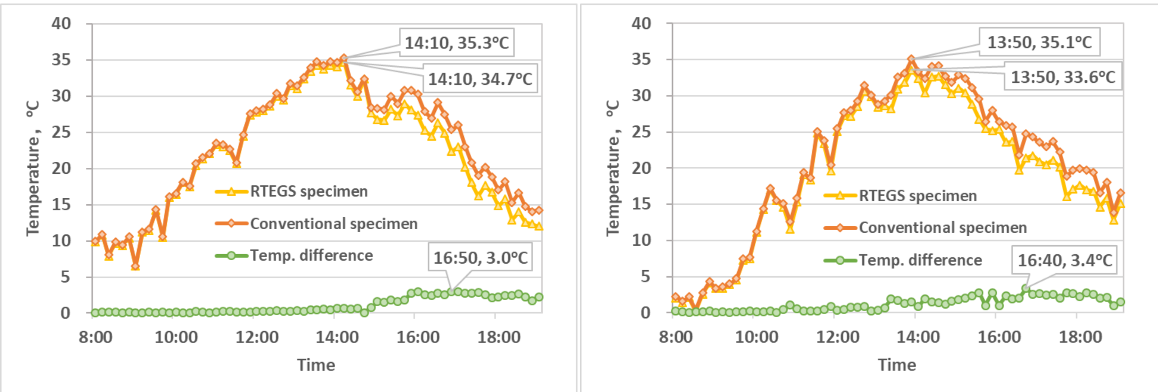

(a) February 24th, 2016. (b) March 22nd, 2017.

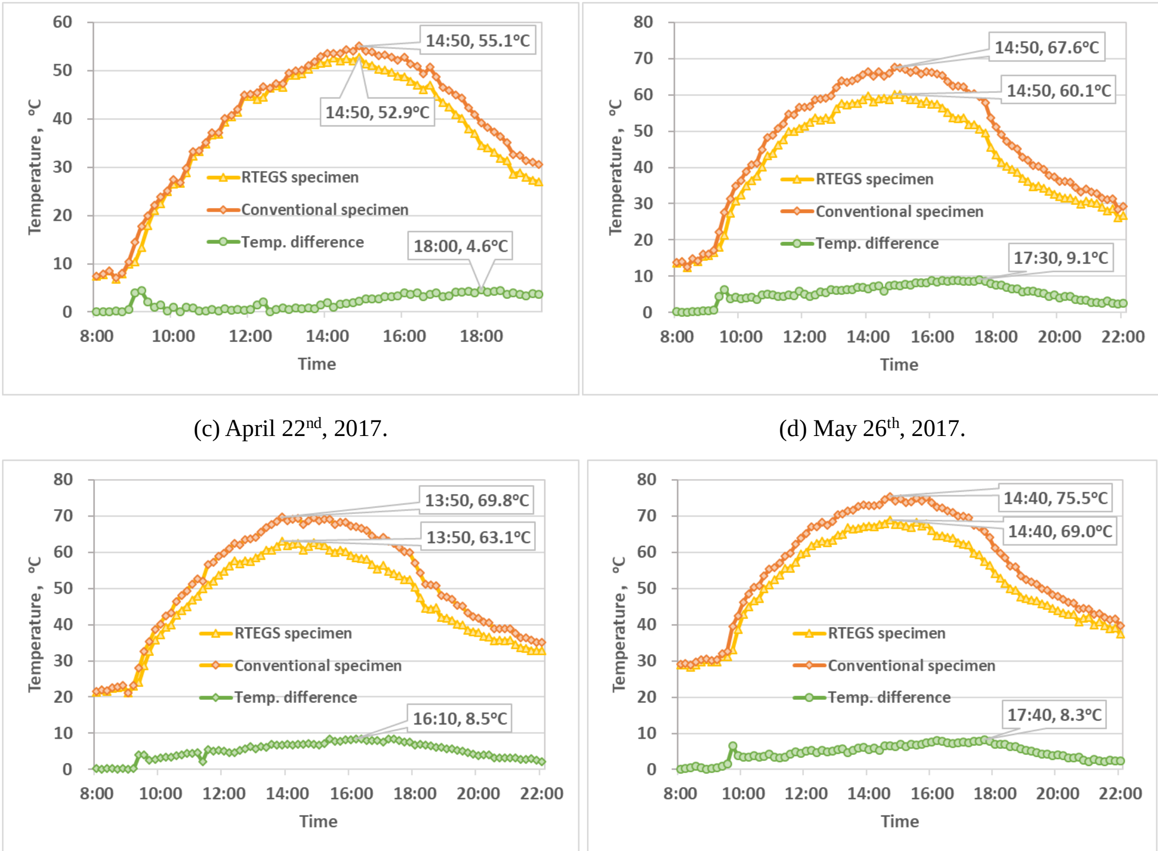

(c) April 22nd, 2017. (d) May 26th, 2017.

(e) June 26th, 2017. (f) July 24th, 2017.

Fig. 8. Temperature of the RTEGS specimen and the conventional specimen in different seasons.

5 Results Analysis

5.1 Influence factors of power-generation

(1) Environmental temperature

The voltage output of the RTEGS specimen changed with the environmental temperature and solar radiation. But the temperature difference between the cold and hot sides of the TEG directly affected the voltage outputs. Fig. 9 illustrates the relationship between the measured voltage outputs and the temperature difference on May 26. The temperature difference is the difference between the temperature of water in the water tank and the surface temperature of the RTEGS specimen. The relationship between the temperature difference and the voltage outputs exhibits two trajectories, both largely linear. This is because the aluminum vapor chambers were embedded in the RTEGS specimen at a depth of 20 mm. The temperature change at this depth lagged behind the temperature changes of the specimen at surface. When the temperature increased, the temperature of the aluminum vapor chamber was lower than the specimen's surface temperature, whereas when the temperature decreased, the temperature of the aluminum vapor chamber was higher than that of the specimen's surface. Therefore, the lower trajectory represents the relationship between the temperature difference and voltage outputs in the temperature-increase process, and the upper trajectory represents the relationship in the temperature-decrease process.

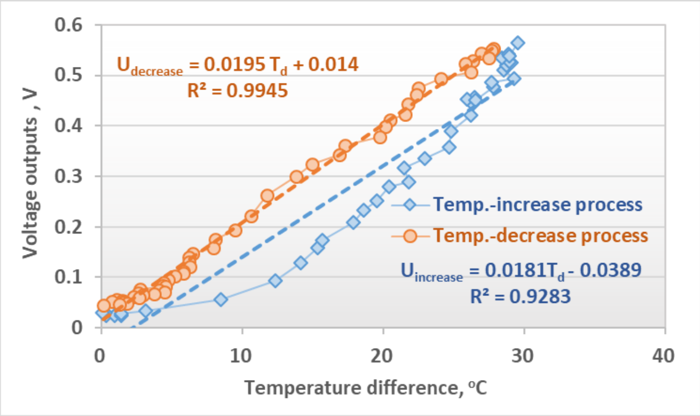

Fig. 9. Relationship between temperature difference and voltage output of RTEGS.

where $U_{increase}$ is the voltage output in the temperature-increase process; $U_{decrease}$ is the voltage output in the temperature-decrease process; T_d is the temperature difference between the specimen surface and water in tank.

(2) Traffic loading

The influence of traffic on power generation is also the focus of study which are two-fold. On the one hand, the influence comes from traffic loading on the devices (aluminum vapor chambers) embedded in the road. Aluminum vapor chambers used in this research can bear a uniform pressure of 4 MPa, which is higher than the loading requirements for traffic. Moreover, no damage was found during the slab specimen (include vapor chambers) compaction, which also proves its adequate bearing capacity. Other materials with good thermal conductivity and bearing strength, such as aluminum and iron, or flexible thermal conductive materials, such as thermal graphite film, can also be considered in subsequent research.

On the other hand, the influence comes from the traffic on power generation efficiency. The power generation efficiency of RTEGS is mainly related to the temperature difference, which is not directly affected by the load from traffic. However, due to the abrasion of black binder and dust deposition, the color of asphalt pavement may turn gray gradually and the temperature of road surface may slightly decrease. To verify this, a comparison test of the temperature of newly formed asphalt mixture specimens and old pavement (open to traffic for about 10 years) was carried out, the results were shown in Fig. 10. The temperature data were obtained by infrared thermal imager and tested on 24th August, 2016. Results showed that, in most of the testing period, surface temperature of the new specimens was slightly higher than the old pavement, but the temperature difference was mostly within 2°C. There was also a small period when the temperature of the old pavement was slightly higher, which is believed to be caused by the heat generated from the friction between the wheel and road surface. However, this amount of heat is relatively small compared with the solar radiation heat, and thus was not considered in the study. Overall, the influence of traffic on power generation is limited.

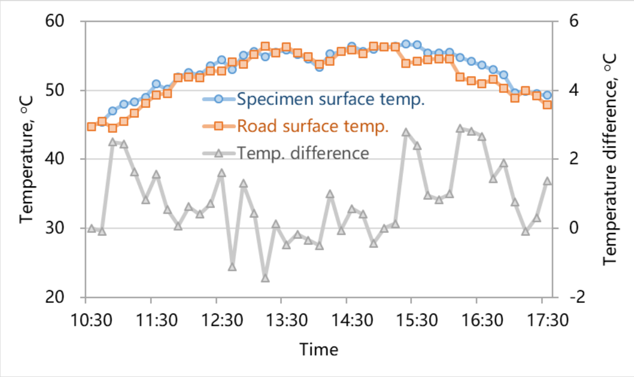

Fig. 10. Temperature of the newly formed asphalt mixture specimens and the old pavement surface.

(3) Scale of experiment

Scale of the RTEGS is another factor affecting the efficiency of power generation. For this reason, indoor tests with the voltage outputs of 1, 2, and 3 pieces of TEG(s) in series were carried out. According to the test results, the voltage output of 3 pieces of TEGs has no significant attenuation. However, when the TEG modules are further increased, the voltage outputs of the system may decrease. Moreover, it is necessary to evaluate the power generation efficiency of different scales through experimental tests in further study.

Results showed that RTEGS had voltage outputs in both summer and winter. The electrical resistance of the TEG was 1.25 Ω at 20–60°C. The electrical current and power generated by RTEGS can be calculated according to Ohm's law. Based on the field data on May 26, the electrical energy generated by the 300 mm × 300 mm RTEGS specimen was approximately 1,080 J. At this rate, an asphalt pavement of 1 km long and 10 m wide can generate approximately 1.2×10^8 J of energy (33 kWh electrical energy) each day without considering the scale effects of RTEGS. The testing site is in a temperate climate. It is foreseeable that the system can be more productive in tropical and subtropical climates that have abundant sunlight and solar heat resources. Through conversion and storage by appropriate electronic instruments, the generated electrical energy can be used for roadside lighting, signals, electronic information boards, communication, nearby residential use, or automobile charging in the future.

5.2 Temperature-reduction analysis

Fig. 11 shows thermal infrared images of the RTEGS specimen and the conventional specimen. The image capture was at 2:50 p.m. on May 26, 2017, which coincided with the peak surface temperature on that day. Fig. 11a shows the surface temperature of the RTEGS specimen; the average temperature was 60.1°C. Fig. 11b shows the surface temperature of the conventional specimen; the average temperature was 67.6°C. There were two obvious temperature ranges in the RTEGS specimen, illustrated as Area 1 and 2 in Fig. 11a. The temperatures of nearly two-thirds of the area with aluminum vapor chambers were lower, with an average of 57.4°C. The average temperature of the remaining area was 63.9°C. The results demonstrated that the aluminum vapor chambers could efficiently transfer heat in asphalt mixtures. The temperature of the pavement implemented with the aluminum vapor chambers was greatly reduced. Due to heat transfer, the temperatures of surrounding areas were also lower than those of conventional pavements.

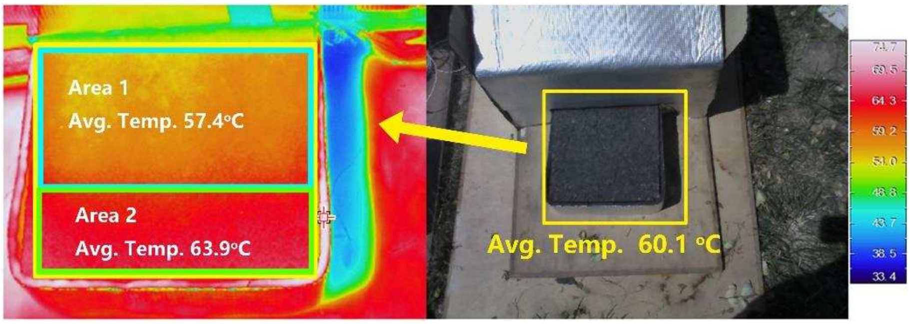

(a) RTEGS specimen.

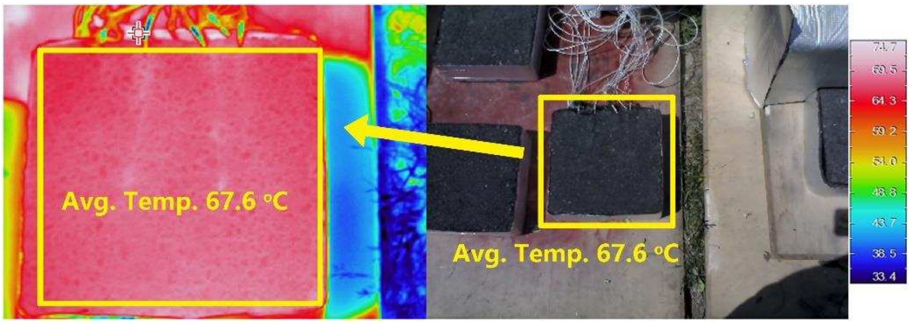

(b) Conventional specimen.

Fig. 11. Surface thermal infrared images of the RTEGS specimen and the conventional specimen (14:50, May 26th, 2017).

Results showed that RTEGS can significantly reduce pavement surface temperature by converting heat to electrical energy. The magnitude of temperature reduction depended on the environmental temperature and solar radiation. Fig. 12 illustrates the relationships between the surface temperature and the temperature reduction in the RTEGS specimen. With the surface temperature increased from 30°C to 60°C, the temperature reduction also increased. In particular, when the surface temperature increased from 50°C to 60°C, the temperature reduction increased from 4°C to 8°C. When the surface temperature further increased from 70°C to 75°C with the increase of environmental temperature and solar radiation, the magnitude of temperature reduction remained constant at 8–9°C. The above results indicate that the temperature reduction by the RTEGS has a limit. This is because the system has limited ability to convert heat to electrical energy. When the available heat energy from the environment is beyond the system's conversion capacity, additional radiation energy will increase the surface temperature of the specimen.

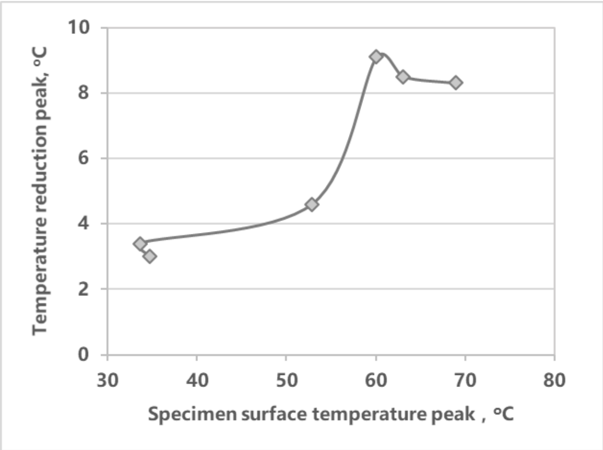

Fig. 12. Relationships between the surface temperature and the temperature reduction of the RTEGS specimen.

5.3 Application prospect

Based on the cost of the current laboratory establishment and the power generation capacity, the direct economic benefit generated by this system is less than the construction cost. The main reason is that the efficiency of the thermoelectric power generation device is relatively low. However, this technology has its prospect of changing the cost-benefit scenarios due to the following reasons. 1）In remote areas far away from power supply facilities, this system can provide sufficient power to meet the energy demand for communication, monitoring and signal transmission on the highway, so as to save the laying and construction cost of the power line; 2) The power generation capability and efficiency in low latitude areas, as well as in areas with abundant sunlight and solar heat resources, are expected to be higher; 3) With the advancement of thermoelectric power generation technology, the power generation efficiency of this system will be improved; 4) In addition to power generation, the reduction in pavement temperature and plastic deformation, as well as the alleviation of urban heat island effect as a result of using RTEGS in cities, have wider and important social benefits which can be quantified in life cycle cost analysis; 5）The system proposed in this paper provides an innovative way of using pavement thermal energy. Further research and industry-scale trial use should be able to improve the power generation efficiency.

6 Conclusion

Asphalt pavements tend to absorb solar energy and accumulate heat in high temperatures during summer, which aggravates pavement rutting, aging of pavement materials, and the urban heat-island effect. A reasonable arrangement of a heat-to-electrical energy conversion module in pavements can partially convert heat absorbed in the pavement to electrical energy, and thus reduce pavement temperatures.

In this study, we designed a new thermoelectric generator (TEG) system for roads. The system transfers pavement heat by aluminum vapor chambers embedded in the pavement, and generates voltage by the TEG making use of the temperature difference between the pavement and the environment. A water tank for temperature reduction was arranged at the cold side of the TEG to increase and maintain the temperature difference. The system provides a new approach to utilizing heat absorbed in asphalt pavement.

Results showed that the surface temperature of the TEG asphalt specimen was significantly lower than that of a conventional asphalt specimen. From June to July (in summer), the system's temperature-reduction peak was approximately 8–9°C, and a temperature reduction of greater than 5°C lasted 7 hours in a day. In February to March (in winter), the temperature reduction of the system was less in both magnitude and duration. These results are compatible with the needs for pavement temperature reduction.

RTEGS can convert pavement heat to electrical energy. Voltage outputs of the RTEGS specimen changed with the environmental temperature and solar radiation. The temperature difference between the cold and hot sides of the TEG directly affected the voltage output. A slab specimen size of 300 mm × 300 m × 100 mm had a voltage peak of 0.564 V on July 24. For comparison, the measured peak value on February 24 was 0.275 V.

Future studies can aim to enhance the heat-to-electrical energy conversion efficiency of the TEG, such as an increase of the temperature difference between the two ends of the TEG, implementation of the new system in a real pavement structure, and to evaluate the impact of traffic loading on its efficiency and durability.

Acknowledgements

This project was jointly supported by the National Natural Science Foundation of China (Grant No. 51608043), the Natural Science Basic Research Plan in Shaanxi Province of China (Grant No. 2015KJXX-23), the Fundamental Research Funds for the Central Universities (Grant No. 310821172001), and the Construction Science and Technology Plan in Shaanxi Province of China (Grant No. 2015-K99).

References

[1] A. Chiarelli, A. Al-Mohammedawi, A. R. Dawson, A. García, Construction and configuration of convection-powered asphalt solar collectors for the reduction of urban temperatures International Journal of Thermal Sciences, 112 (2017) 242-251

[2] Abbas Mohajerani, Jason Bakaric, Tristan Jeffrey-Bailey, The urban heat island effect, its causes, and mitigation, with reference to the thermal properties of asphalt concrete, J. Environ. Manage.197 (2017) 522-538.

[3] Joe Arnaldo Villena Del Carpio, Deivis Luis Marinoski, Glicério Trichês, Urban pavements used in Brazil: Characterization of solar reflectance and temperature verification in the field, Solar Energy, 134 (2016) 72–81.

[4] Federico Rossi, Beatrice Castellani, Andrea Presciutti, Experimental evaluation of urban heat island

mitigation potential of retro-reflective pavement in urban canyons, Energy Build. 126 (2016) 340–352.

[5] Hashem Akbari a, Dionysia Kolokotsa, Three decades of urban heat islands and mitigation technologies research, Energy Build. 133 (2016) 834–842.

[6] Nickholas Anting, Mohd. Fadhil Md. Din, Kenzo Iwao, Experimental evaluation of thermal performance of cool pavement Material using waste tiles in tropical climate, Energy Build. 142 (2017) 211–219.

[7] Jiachuan Yang, Zhi-Hua Wang, Kamil E. Kaloush, Effect of pavement thermal properties on mitigating urban heat islands: A multi-scale modeling case study in Phoenix, Build. Environ. 108(2016) 110-121.

[8] Haley E. Gilbert, Pablo J. Rosado, George Ban-Weiss, Energy and environmental consequences of a cool pavement campaign, Energy Build. 2017.

[9] Du Yinfei, Shi Qin, Wang Shengyue, Highly oriented heat-induced structure of asphalt pavement for reducing pavement temperature, Energy Build. 85 (2014) 23–31.

[10] Du Yinfei, Wang Shengyue, Zhang Jian, Cooling asphalt pavement by a highly oriented heat conduction structure, Energy Build. 102 (2015) 187–196.

[11] J. Antonio Ramos García, María Castro, Analysis of the temperature influence on flexible pavement deflection, Constr. Build. Mater. 25 (2011) 3530–3539.

[12] Dahae Kim, Y. Richard Kim, Development of Stress Sweep Rutting (SSR) test for permanent deformation characterization of asphalt mixture, Constr. Build. Mater. 154 (2017) 373–383.

[13] H.K. Salama, K. Chatti, Evaluation of fatigue and rut damage prediction methods for asphalt concrete pavements subjected to multiple axle loads, International Journal of Pavement Engineering, 12 (2017) 25-36.

[14] Farhad Yousefi Rad, Michael D. Elwardany, Cassie Castorena, Investigation of proper long-term laboratory aging temperature for performance testing of asphalt concrete, Constr. Build. Mater. 147 (2017) 616–629.

[15] Fan Yin, Edith Arámbula-Mercado, Amy Epps Martin Long-term ageing of asphalt mixtures, Road Materials and Pavement Design, 18 (2017) 2-27.

[16] Ilaria Menapace , Wubulikasimu Yiming, Eyad Masad. Chemical analysis of surface and bulk of asphalt binders aged with accelerated weathering tester and standard aging methods, Fuel, 202 (2017) 366-379.

[17] Hassan Radhi, Essam Assem, Stephen Sharples, On the colors and properties of building surface materials to mitigate urban heat islands in highly productive solar regions, Build. Environ. 72 (2014) 162-172.

[18] W. Jiang, A.M. Sha, J.J. Xiao, Y. L. Li, Y. Huang, Experimental study on filtration effect and mechanism of pavement runoff in permeable asphalt pavement, Constr. Build. Mater. 100 (2015) 102–110.

[19] Federica Rosso, Anna Laura Pisello, Franco Cotana, On the thermal and visual pedestrians' perception about cool natural stones for urban paving: A field survey in summer conditions, Build. Environ. 107 (2016) 198-214.

[20] X. Cao, B. Tang, H. Zhu, et al., Cooling principle analyses and performance evaluation of heat-reflective coating for asphalt pavement, J. Mater. Civ. Eng. 23 (7) (2010) 1067–1075.

[21] Hashem Akbari, H. Damon Matthews, Global cooling updates: Reflective roofs and pavements, Energy Build. 55 (2012) 2–6.

[22] W. Jiang, A.M. Sha, J.J. Xiao, Z.J. Wang, Alex Apeagyei, Experimental study on materials

composition design and mixture performance of water-retentive asphalt concrete, Constr. Build. Mater. 111 (2016) 128–138.

[23] Jingjing Xiao, Wei Jiang, Dongdong Yuan, Aimin Sha & Yue Huang, Effect of styrene–butadiene rubber latex on the properties of modified porous cement-stabilised aggregate, Road Materials and Pavement Design, (2017), DOI: 10.1080/14680629.2017.1337042.

[24] E. Toraldo, E. Mariani, S.Alberti, M. Crispino, Experimental investigation into the thermal behavior of wearing courses for road pavements due to environmental conditions. Constr. Build. Mater. 98 (2015) 846-852.

[25] A. Karasawa, K. Toriiminami, N. Ezumi, K. Kamaya, Evaluation of performance of water-retentive concrete block pavements. 8th International Conference on Concrete Block Paving, San Francisco, California USA, 6-8, November 2006.

[26]H. Yamagata, M. Nasu, M. Yoshizawa, A. Miyamoto, M. Minamiyama, Heat island mitigation using water retentive pavement sprinkled with reclaimed wastewater. Water Science & Technology, 57 (2008) 763-71.

[27] Chrysanthi Efthymiou, Mat Santamouris, Dionysia Kolokotsa, Development and testing of photovoltaic pavement for heat island mitigation, Solar Energy, 130 (2016) 148–160.

[28] M. Santamouris, N. Gaitani, A. Spanou, Using cool paving materials to improve microclimate of urban areas - Design realization and results of the flisvos project, Build. Environ. 53 (2012) 128-136.

[29] Francisco Duarte, Adelino Ferreira, Energy harvesting on road pavements: State of the art, Proceedings of the ICE-Energy, March 2016.

[30] Ali Azhar Butt, Susanna Toller, Bjorn Birgisson, Life cycle assessment for the green procurement of roads: a way forward, Journal of Cleaner Production, 90 (2015) 163-170.

[31] Feng Chen, Nathaniel Taylor, Nicole Kringos, Electrification of roads: Opportunities and challenges, Applied Energy, 150 (2015) 109–119.

[32] Wei Jiang, Dongdong Yuan, Shudong Xu, Huitao Hu, Jingjing Xiao, Aimin Sha, Yue Huang, Energy harvesting from asphalt pavement using thermoelectric technology, Applied Energy, 205(2017): 941–950.

[33] Vanesa Bobes-Jesus, Pablo Pascual-Muñoz, Daniel Castro-Fresno, Asphalt solar collectors: A literature review, Applied Energy. 102 (2013) 962–970.

[34] W. Kang-Won, A. J. Correia, A Pilot Study for Investigation of Novel Methods to Harvest Solar Energy from Asphalt Pavements, Korea Institute of Construction Technology (KICT), Goyang City, South Korea, 2010.

[35] Z. Zhou, X. Wang, X. Zhang, Effectiveness of pavement solar energy system–an experimental study, Applied Energy. 138 (2015) 1-10.

[36] SR (Solar Roadways), (Accessed 06 February 2017), http://www.solarroadways.com .

[37] TNO. SolaRoad: paving the way to the roads of the future, (Accessed 06 February 2017) https://www.tno.nl/media/4574/solaroadtechnology.pdf.

[38] F. Duarte, A. Ferreira, Energy harvesting on road pavements: state of the art, Proceedings of the ICE-Energy. 169 (2016) 79–90.

[39] A. Dawson, R. Mallick, A. G. Hernandez, P. K. Dehdezi, Energy Harvesting from Pavements. Green Energy and Technology, Springer Press, 2014.

[40] Sullivan, C., de Bondt, A. H., Jansen, R., & Verweijmeren, H. Innovation in the production and commercial use of energy extracted from asphalt pavements. 6th Annual International Conference on Sustainable Aggregates, International Journal of Pavement Engineering and Asphalt

Technology, 8(2017). Liverpool.

[41] Hasebe M, Kamikawa Y and Meiarashi S. Thermoelectric generators using solar thermal energy in heated road pavement. In Proceedings ICT ’06 – 25th International Conference on Thermoelectrics (ICT), Vienna, Austria. IEEE – Institute of Electrical and Electronics Engineers, New York, NY, USA, 2006: 697-700.

[42] Weather China: Climate of Xi'an City, Shaanxi, (Accessed 06 Janurary 2018) http://www.weather.com.cn/cityintro/101110101.shtml.